UBVRI PHOTOMETRY OF BETELGEUSE OVER 23 YEARS SINCE 1999

Yojiro Ogane[1], Osamu Ohshima[2,3], Daisuke Taniguchi[4], and Naohiro Takanashi[5]

1) Ogane Hikari Observatory, 3-28-29 Hikari, Kokubunji, Tokyo 185-0034, Japan, hqk00742@nifty.com

2) Okayama University of Science, 1-1 Ridaicho, Kita-ku, Okayama, Okayama 700-0005, Japan

3) Ohshima Tamashima Observatory, 3-10-15 Tamashima, Kurashiki, Okayama 713-8102, Japan, o2@otobs.org

4) Department of Astronomy, The University of Tokyo, 7-3-1 Hongo, Bunkyo-ku, Tokyo 113-0033, Japan, d.taniguchi.astro@gmail.com

5) Executive Management Program, The University of Tokyo, 7-3-1 Hongo, Bunkyo-ku, Tokyo 113-8654, Japan, naohiro.takanashi@emp.u-tokyo.ac.jp

Abstract: We report the results of our continuous $UBVRI$-band photometry of Betelgeuse from 1999 to 2022 using the same photometric system. There are two advantages in our observation: (1) we used a photodiode as a detector to avoid saturation, and (2) our data set includes U-band light curve, which is not widely observed in recent CCD photometries. Using our light curves, we conducted the periodicity analysis, and found ∼405- and ∼2160-day periods. We also discuss the tentative detection of a long-period variation over 20 years or longer. Finally, we discuss the peculiar variation of the $U - B$ color index during the "Great Dimming" event between late 2019 and early 2020.

1 Introduction

Located at the Orion's shoulder, Betelgeuse is one of the nearest red supergiant stars, and is also known as a semi-regular variable (Lloyd, 2020). In 1980s, when this project was initiated, there was an active discussion on the variable period(s) of Betelgeuse (see Dupree et al., 1987, and references therein), and an emergence of a long-term, homogeneous photometric dataset was anticipated. Under such circumstance, we started to investigate the photometric periodicity of Betelgeuse by performing accurate, multi-color photometry with the same photometric system over tens of years.

Nowadays, thanks to many variable-star observers worldwide contributing to the American Association of Variable Star Observers (AAVSO) database, the variable periods of Betelgeuse in the visible band has been well measured: e.g., 185±13.5, 416±24, and 2365±10 days (Joyce et al., 2020). Even in such an era, a long-term observing campaign by a specific observer would be valuable, considering that such data set like the AAVSO database cannot, by definition, circumvent systematic biases among the photometric data provided by multiple observers.

In addition, starting from the latter half of 2019, so-called "Great Dimming" event occurred (Guinan et al., 2020; Dupree et al., 2022), and many well-established telescopes pointed towards Betelgeuse. However, the cause of the Dimming is still under debate (Montargès et al., 2021). Proposed explanations include, for example, a decrease in the effective temperature (e.g. Harper et al., 2020), an increase in the (circumstellar) dust extinction (e.g. Dupree et al., 2020), and both of them (e.g. Levesque & Massey,

Table 1: *UBVRI* bandpass of the Ogane's photometric system. Full table is available on the OEJVS's web site (https://oejv.physics.muni.cz/issues/table1_0233.txt) and also on the authors' web site (http://hikariao.la.coocan.jp/figure.html).

Wavelength [Å]	U	B	V	R	I
3050	0.0000	0.0000	0.0000	0.0000	0.0000
3100	0.0001	0.0000	0.0000	0.0000	0.0000
3150	0.0036	0.0000	0.0000	0.0000	0.0000
3200	0.0218	0.0000	0.0000	0.0000	0.0000
...					

2020). One can also interpret the observational evidences as consequences of a surface mass ejection (Dupree et al., 2022).

In this paper, we present our *UBVRI* multi-band photometry of Betelgeuse over 23 years, and determine the variable periods for the V band. Moreover, with the aid of the long-term, multi-band nature of our dataset, especially the inclusion of the U band, we discuss a possible cause of the Great Dimming.

2 Observation

2.1 Observation and basic reduction

We have been observing Betelgeuse in the *UBVRI* bands since 1999 at the private Ogane Hikari Observatory located in Hikari-cho, Kokubunji City, Tokyo, Japan (139.4°E, 35.7°N). In total, we here present data for 572 nights, including 17 nights in which we observed Betelgeuse twice per night. We used a 25 cm-aperture, f/8 Newtonian telescope until February 2006, and used a 30 cm-aperture, f/16 Cassegrain telescope after that. In order to avoid saturation for very bright stars like Betelgeuse, we used a photodiode (Hamamatsu S1226-5BQ), instead of photomultiplier, as a detector to conduct a single-channel, photoelectric observation.

To build a photometric system imitating the standard Johnson's *UBVRI* system (Johnson, 1965), we stacked a few commercially-available colored-glass filters for each band. The resultant bandpass for each band, i.e. the combination of the photodiode's sensitivity and filters' throughputs, is showed in Figure 1 and Table 1. There are some discrepancies between the Ogane's and Johnson's system. For example, the effective wavelength of the Ogane's B band is slightly longer than the Johnson's one, and the band width is narrower. Because of these discrepancies in the photometric bands, we distinguish the Ogane's system from the standard Johnson's system by adding "og" subscripts, if necessary.

We used the all-sky photometry method (Henden & Kaitchuck, 1982) for the photometry. The differential photometry method cannot be used for our case because no star around Betelgeuse is suitable as a comparison star in terms of its brightness and color. As the candidate standard stars for the all-sky photometry, we selected 83 stars from the Arizona-Tonantzintla catalog (Iriarte et al., 1965), with the main criteria being (1) non-variable stars and (2) the V magnitude of 4.5 or brighter. In each night, 10–12 stars
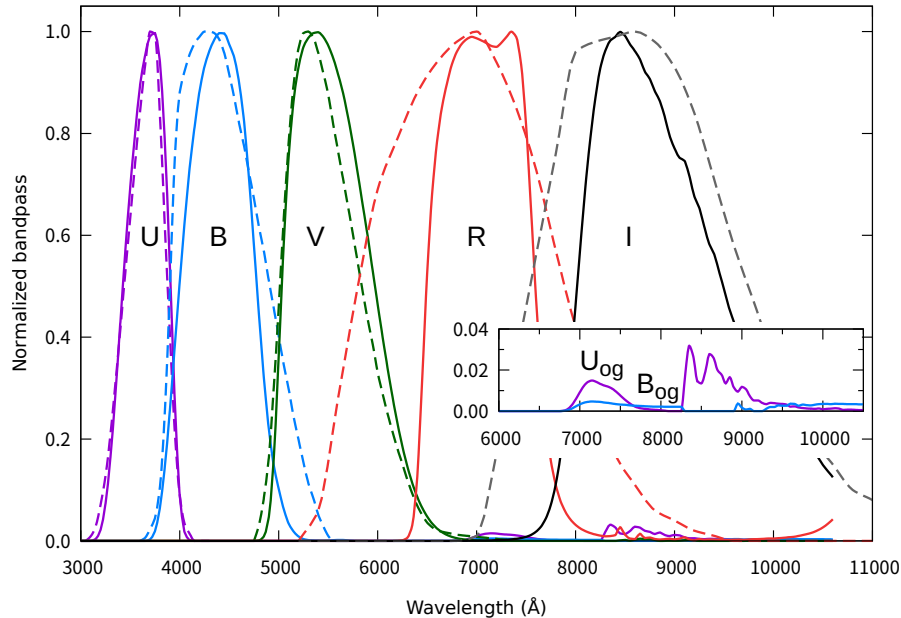
Figure 1: Normalized bandpass of $UBVRI$ systems. Solid and dashed lines represent Ogane's and standard Johnson (1965) systems, respectively. In the long wavelength side ($\lambda > 7000\,\text{Å}$), there are small red leakage to the U and B bands, which has a non-negligible effect to the photometry of Betelgeuse (see the main text).

among them with the altitudes higher than $30°$ were observed.

Each object among photometric standard stars and Betelgeuse was observed typically once per night for each band. The typical integration time for the standards was 80–100 s for each of the $BVRI$ bands and 200–400 s for the less sensitive U band. For Betelgeuse, which is brighter than most of the standards, we used 80–90 s integration for all the bands. In total, one set of the observations of standard stars and Betelgeuse took about 5 hours. Due to this long time of integrations required for each night, photometric errors because larger when the weather was unstable.

For each night's data set, we performed a multivariate analysis to determine the extinction coefficients of the telluric atmosphere and transformation coefficients from the natural- to the standard-system V magnitude and colors. Since our list of standard stars does not include stars as red as Betelgeuse, we extrapolated the relation between observed raw counts and the magnitudes calibrated with the standard system before applying to Betelgeuse. This extrapolation could introduce systematic bias/errors to the measured photometric magnitudes, but we found no detectable systematic errors that depend on the color or airmass of an object. Note that we removed seven observations with poor weather conditions from our published photometric catalog.
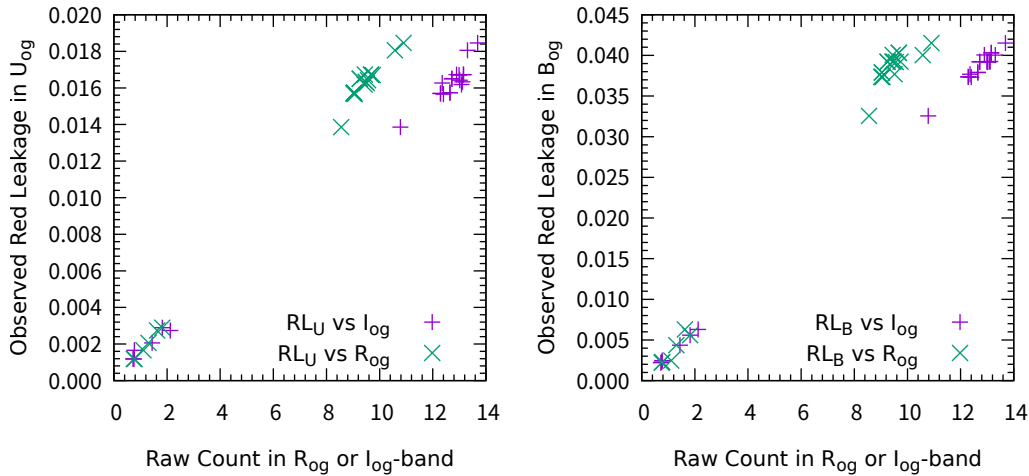
Figure 2: Red leakage in U_{og} (left panel) and B_{og} (right panel) bands vs R_{og} (green cross) and I_{og} (purple plus) raw counts. Data points at the top right corners, i.e. those with the x-axis values larger than 8, show the results for Betelgeuse observed on different nights, and are used for the fitting.

2.2 Correction for red leakage

A small portion of red and near-infrared photons passes through the blue (U_{og} and B_{og}) filters, as shown in Figure 1. This red leakage has a non-negligible effect to our photometry, especially for M-type stars; for example, the uncorrected U_{og}-band flux of Betelgeuse is contributed almost the same amounts by U-band and RI-band photons.

In order to investigate the effect of the red leakage to our photometry, we measured, in summer 2021, the amounts of raw $U_{\mathrm{og}}B_{\mathrm{og}}$ counts contributed by red photons. For this purpose, we inserted a red filter transparent at wavelengths longer than 6500 Å into each of the U_{og}- and B_{og}-band filter systems. Then, we observed Betelgeuse for multiple times and also some other red stars with these stacked filters. Figure 2 shows the correlations between the amount of the red leakage and the amount of the raw count in the R_{og} and I_{og} bands. We fitted these data, only of Betelgeuse, using linear regression, and obtained the following equations to best correct for the red leakage:

$$B_{\mathrm{count}} = B_{\mathrm{raw}} - ((3.27 \times 10^{-3})I_{\mathrm{raw}} - (2.38 \times 10^{-4})R_{\mathrm{raw}} - 7.44 \times 10^{-4})/0.895, \quad (1)$$

$$U_{\mathrm{count}} = U_{\mathrm{raw}} - ((7.63 \times 10^{-4})I_{\mathrm{raw}} + (9.97 \times 10^{-4})R_{\mathrm{raw}} - 2.77 \times 10^{-4})/0.895. \quad (2)$$

Here, the subscript "raw" indicates the raw count for each band before the atmospheric correction, and "count" indicates the counts after correcting the red leakage. The constant 0.895 is the transmittance at red wavelengths of the inserted red filter. These equations are related to the ratios of the throughputs between the RI and UB filters in red wavelength ranges, and thus expected to be independent of the used telescopes. In other words, although these equations are determined using the new 30 cm telescope, they are expected to be applicable to the photometric data obtained with the old 25 cm telescope.
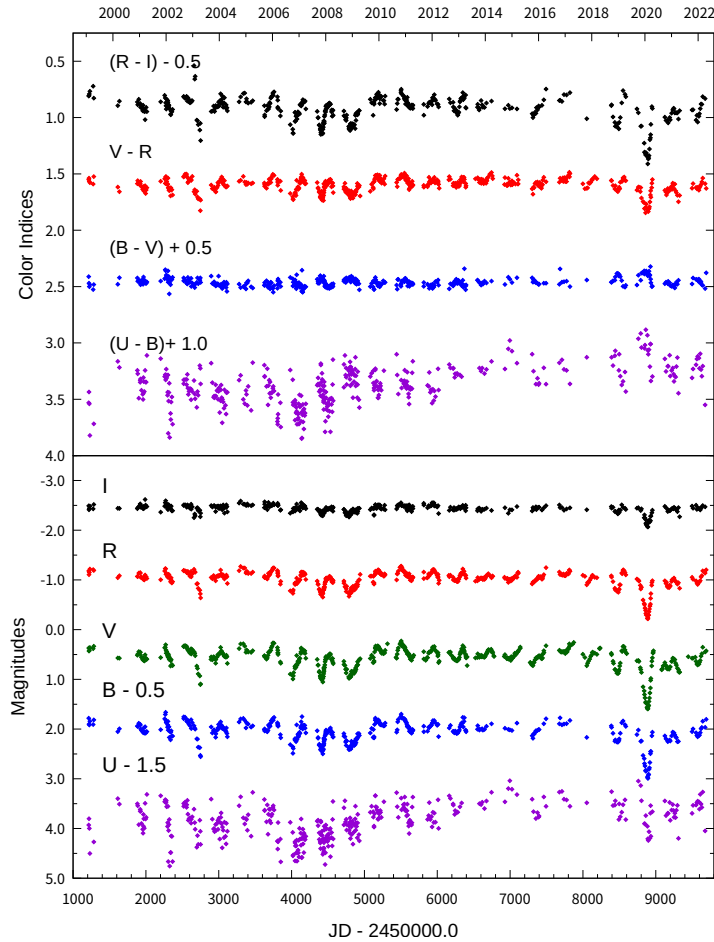
Figure 3: Magnitude and color variations of Betelgeuse from 1999 to 2022. Upper panel: color indices of $U - B$, $B - V$, $V - R$, and $R - I$. Lower panel: $UBVRI$ magnitudes.

We corrected U_{og} and B_{og} data observed before summer 2021 using the $R_{\mathrm{og}}I_{\mathrm{og}}$-band counts using these equations. For the observations after autumn 2021, we measured and subtracted the red leakage in U_{og} and B_{og} using the red filter. Note that even after the correction for the red leakage by this procedure and the transformation to the standard system, we cannot eliminate a possible systematic bias of our $U_{\mathrm{og}}B_{\mathrm{og}}$ photometry compared to the Johnson's system due to, e.g., the different filter transmissions and an imperfect correction of the red leakage.

Table 2: *UBVRI* photometry of Betelgeuse by Ogane. Full table is available on the OEJVS's web site (https://oejv.physics.muni.cz/issues/table2_0233.txt) and also on the authors' web site (http://hikariao.la.coocan.jp/data.html).

Hel.J.D.	V	err	$U-B$	err	$B-V$	err	$V-R$	err	$R-I$	err
2451215.04	0.369	0.043	2.531	0.072	1.912	0.037	1.551	0.022	1.309	0.014
2451217.98	0.431	0.041	2.436	0.042	1.970	0.017	1.538	0.013	1.306	0.016
2451224.05	0.416	0.013	2.541	0.025	2.001	0.007	1.567	0.010	1.291	0.018
2451231.05	0.359	0.011	2.822	0.120	1.984	0.014	1.578	0.013	1.267	0.013
2451275.98	0.382	0.010			2.026	0.010	1.590	0.008	1.222	0.021
2451284.96	0.334	0.015	2.718	0.111	1.982	0.021	1.524	0.020	1.328	0.036
2451613.96	0.571	0.020	2.164	0.068	1.980	0.027	1.617	0.025	1.394	0.017
2451635.97	0.574	0.015	2.218	0.099	1.921	0.033	1.658	0.016	1.355	0.028
2451883.15	0.515	0.013	2.244	0.026	1.924	0.011	1.587	0.017	1.362	0.017
2451888.15	0.494	0.019	2.274	0.035	1.953	0.007	1.560	0.018	1.386	0.015
...										

3   Results and discussion

3.1   Time variation of the magnitudes and color indices

The resultant magnitudes and color indices of Betelgeuse for each night are shown in Figure 3 and Table 2. The "err" columns in Table 2 show the standard deviation of the residuals around the multivariate regressions for correcting the atmospheric extinction and photometric-system differences using the standard stars' data.

The periodicity in the obtained V-band light curve was analyzed using Period04 code[1] (Lenz & Breger, 2005). We detected mainly three period components: ∼2160, ∼405, and ∼202 days, probably corresponding to the long secondary period (LSP), fundamental mode pulsation, and first harmonics of the fundamental mode, respectively (Figure 4). The errors in measuring peak frequencies in the power are several days for the longest period and smaller than one day for the others. Although these measurement errors would be smaller than the uncertainties of "physical" periods (Kiss, Szabó & Bedding, 2006), our determined periods are within, or at least near to, the ranges of previous measurements by Kiss, Szabó & Bedding (2006); Joyce et al. (2020), which supports the reliability of our period determination.

We have also examined the long-term variation of Betelgeuse, especially in the $U-B$ color index. Johnson et al. (1966) reported multi-band photometry of Betelgeuse during the 2-year duration starting from JD = 2438315 (i.e. October 1963). For the V magnitude and $U-B$ color, they observed Betelgeuse for eight epochs. There is a gap of about 35 years between the Johnson's observations and ours, and we could not find any published $U-B$ measurements during this gap. Plotting Johnson's and our $U-B$ data (lower panel of Figure 5), we found a long-term variation in the $U-B$ color, possibly with a period of ∼27 years. Such long-timescale variation is also seen in the AAVSO's V-band light curve (e.g. Montargès et al., 2021), and it is possibly due to the rotational
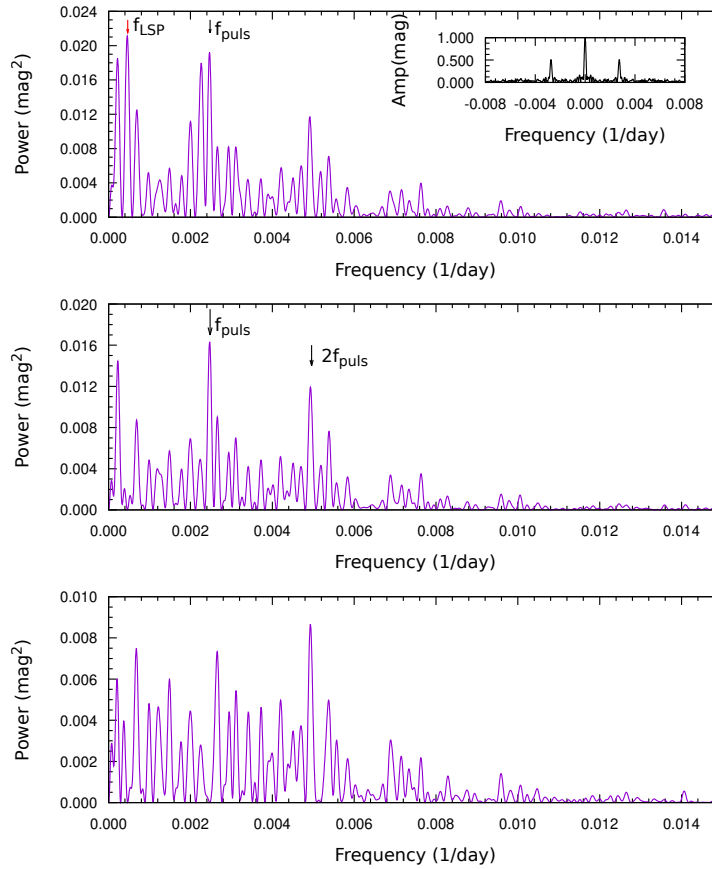
---

[1]https://univie.ac.at/tops/Period04/

Figure 4: The top panel shows the power spectrum of our V-band light curve. The strongest frequency, i.e., the long-secondary period f_{LSP} (LSP), is indicated by the red arrow. The inset shows the spectral window function of the data. The middle panel shows the power spectrum after removing the LSP signals. The peaks corresponding to the fundamental model pulsation (f_{puls}) and its first harmonic ($2f_{\mathrm{puls}}$) are indicated by the black arrows. The bottom panel shows the residual spectrum after removing the aforementioned frequencies.

modulation (Joyce et al., 2020) considering the rotational period of $\sim$31 years (Kervella et al., 2018). Thus, the long-term $U - B$ variation that we found might be attributed to an actual variation of Betelgeuse over the 35-year gap, at least in part, rather than the systematic bias and/or errors. This is also supported by the fact that the synthesized and extrapolated $U - B$ light curve using only Ogane's data (blue thin line in the lower panel of Figure 5) well predicts the Johnson et al. (1966) data points. In addition, we found that the V-band variation (upper panel of Figure 5) is weaker than the $U - B$ color one. Nevertheless, possible systematic bias between the two observers, i.e., we and Johnson et al. (1966), should be kept in mind. Future longer-term, continuous observations will be required to further examine these longer period phenomena.
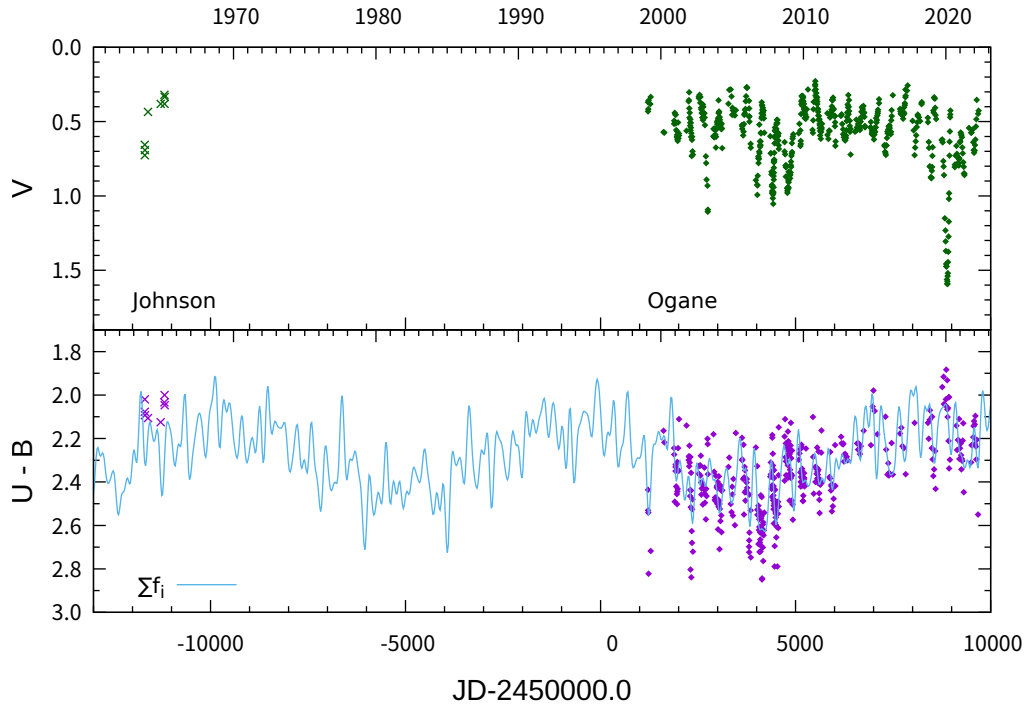
Figure 5: Long-term V and $U - B$ variation of Betelgeuse. Dots and crosses represent the data measured by this work and by Johnson et al. (1966), respectively. There are two type of variations: the pulsation with the $\sim$400-day period and long-term variation with the time scale of a few tens of years. Blue thin line in the lower panel shows the synthesized light curve using top ten Fourier components of the Ogane's data points; we do not include Johnson et al. (1966) data points in this Fourier transformation.

3.2 Color-magnitude diagram: peculiar behavior of the $U - B$ color during the Great Dimming

During the usual phases of Betelgeuse, i.e. excluding the Great Dimming phase from late 2019 to early 2020, the color indices and the V magnitude that we measured exhibit good correlations, especially for the $B - V$, $V - R$, and $R - I$; when the V magnitude is lower than the average, $V - R$ and $R - I$ colors are redder and $U - B$ and $B - V$ colors are bluer (Figure 6). These correlations could be mainly attributed to the variation in the effective temperature, considering the dependence on the temperature of the black body shape and of the strengths of the TiO molecular bands in the BVR bands (McKemmish et al., 2019), latter of which are very sensitive to the effective temperature (Levesque et al., 2005).

The scatter around the relation between V and $U - B$ is larger than the observational error for $U - B$ quoted in Table 2. To reveal the origin of this scatter, we plotted the long-term change in the trajectory between $U - B$ and V of the individual 400-day cycle (Figure 7). As a result, we found differences in the trajectories between different cycles. For example, in the 2003 cycle (i.e. late 2003–early 2004), which is the second largest dimming event during our observation after the Great Dimming, the average color index
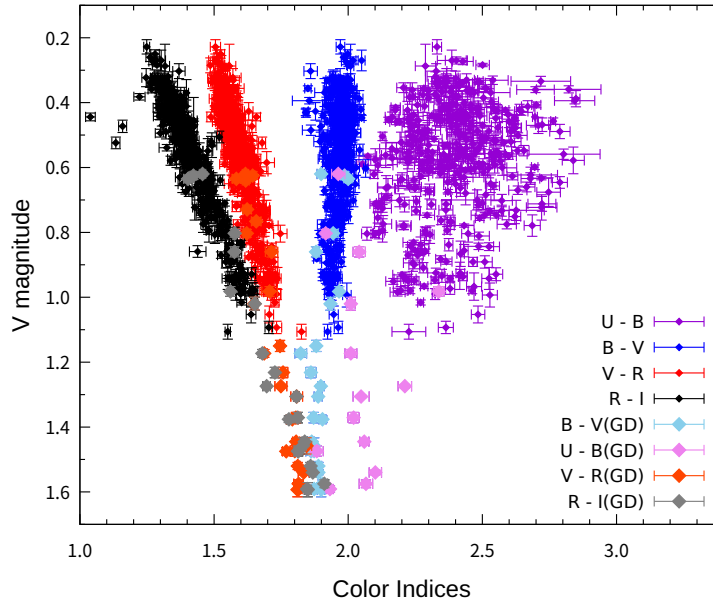
Figure 6: Color-magnitude diagrams of our photometric data set. Small and large symbols represent the data during and outside the Great Dimming, respectively.

is $U - B \sim 2.5$. In contrast, during the Great Dimming period, the average color index is bluer, $U - B \sim 2.0$. These differences suggest that not only the effective temperature and dust extinction but also the chromospheric activity (Davies & Plez, 2021) may affect the $U - B$ color. Therefore, the large scatter might not be observational systematic errors, but rather than the actual variation of the spectral-energy distribution of Betelgeuse.

Focusing onto the Great Dimming, the trajectory on the color-magnitude diagram between $U - B$ and V exhibited unusual behavior: the color remained mostly unchanged, or even became redder when the V-magnitude is fainter (right panel of Figure 7). Considering that the temperature was decreased by ~ 100 K during the Dimming (e.g. Levesque & Massey, 2020; Taniguchi et al., 2022), which makes the $U - B$ color ~ 0.2 mag bluer, effect(s) that makes the color redder should have happened. Plausible scenarios include the increased circumstellar extinction (Montargès et al., 2021; Taniguchi et al., 2022).

Moreover, when the V magnitude was staying at the minimum of ~ 1.6 mag on February 2020, $U - B$ became redder and $B - V$ did slightly bluer by ~ 0.2 and $\lesssim 0.1$ mag, respectively. These variations in the colors, without variation in the V magnitude, could be explained, for example, assuming that the following three phenomena occurred in succession. First, the chromosphere experienced an increased activity during the second half of 2019, i.e., only before the Great Dimming (Dupree et al., 2020). Second, the dust extinction was enhanced for about half a year, and it reached its maximum before the Dimming on February 2020 (Taniguchi et al., 2022). Finally, the surface temperature was cooler than the usual for about half a year, and it reached its minimum after the Dimming (Kravchenko et al., 2021).
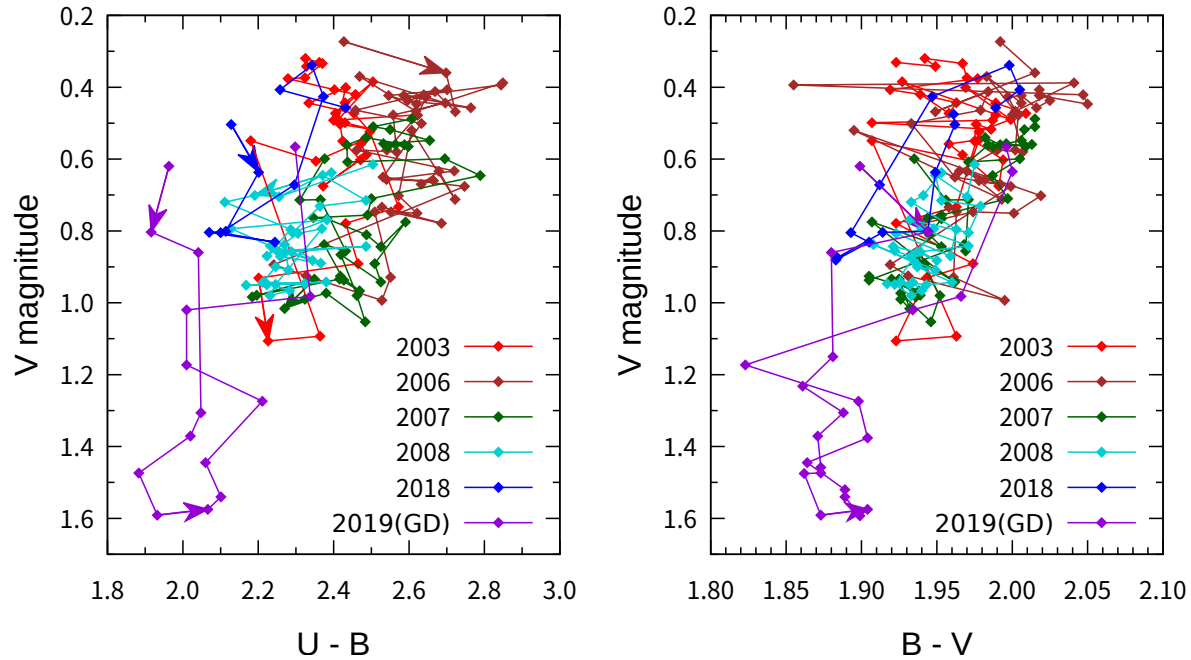
9

Figure 7: The color-magnitude diagram between the V magnitude and $U - B$ color index for some variability cycles, including the Great Dimming (GD) phase in 2019.

References

Davies, B., & Plez, B. 2021, *MNRAS*, **508**, 5757, 2021MNRAS.508.5757D

Dupree, A. K., et al. 1987, *ApJL*, **317**, L85, 1987ApJ...317L..85D

Dupree, A. K., et al. 2020, *ApJ*, **899**, 68, 2020ApJ...899...68D

Dupree, A. K., et al. 2022, *ApJ*, **936**, 18, 2022ApJ...936...18D

Guinan, E., et al. 2020, *ATel*, **13512**, 1, 2020ATel13512....1G

Harper, G. M., et al. 2020, *ApJ*, **905**, 34, 2020ApJ...905...34H

Henden, A. A., & Kaitchuck, R. H. 1982, Astronomical photometry, 1982asph.book.....H

Herschel, J. F. W. 1840, *MmRAS*, **11**, 269, 1840MmRAS..11..269H

Hoffleit, D., & Jaschek, C. 1991, The Bright Star Catalogue, 5th rev. ed., 1991bsc..book.....H

Iriarte, B., et al. 1965, *Sky and Telescope*, **30**, 21, 1965S%26T....30...21I

Johnson, H. L. 1965, *ApJ*, **141**, 923, 1965ApJ...141..923J

Johnson, H., et al. 1966 Communications of the Lunar and Planetary Laboratory No. 63 Vol. 3 Part 3, Table 4 p.12

Joyce, M., et al. 2020, *ApJ*, **902**, 63, 2020ApJ...902...63J

Kervella, P., et al. 2018, *A&A*, **609**, A67, 2018A%26A...609A..67K

Kiss, L. L., Szabó, Gy. M., & Bedding, T. R. 2006, *MNRAS*, **372**, 1721, 2006MNRAS.372.1721K

Kravchenko, K., et al. 2021, *A&A*, **650**, L17, 2021A%26A...650L..17K

Lenz, P., & Breger, M. 2005, *CoAst*, **146**, 53, 2005CoAst.146...53L

Levesque, E. M., et al. 2005, *ApJ*, **628**, 973, 2005ApJ...628..973L

Levesque, E. M., & Massey, P. 2020, *ApJL*, **891**, L37, 2020ApJ...891L..37L

Lloyd, C. 2020, *BAAVC*, **184**, 22, 2020BAAVC.184...22L

McKemmish, L. K., et al. 2019, *MNRAS*, **488**, 2836, 2019MNRAS.488.2836M

Montargès, M., et al. 2021, *Nature*, **594**, 365, 2021Natur.594..365M

Taniguchi, D., et al. 2022, *Nature Astronomy*, **6**, 930, 2022NatAs...6..930T